nanoDDS
14th INTERNATIONAL NANOMEDICINE & DRUG DELIVERY SYMPOSIUM

MODELING SPATIOTEMPORAL DISTRIBUTION OF THE [18F]-FMISO PET TRACER IN TUMOR IMAGING

M. Soltani[1,2,3], Sh. Shahriyari[4], A. Soltani Goharrizi[4], A. Rahmim[2].
[1] *Department of Mechanical Engineering, KNT University of Technology, Tehran, Iran*
[2]*Department of Radiology and Radiological Science, School of Medicine, Johns Hopkins University, Baltimore, MD, United States*
[3]*Department of Computational Medicine Institute at KNT University of Technology, Tehran, Iran*
[4]*Departmant of Chemichal Engineering, Faculty of Engineering, Shahid Bahonar University of Kerman, Kerman, Iran*

Background and Objectives

- [18F]-FMISO PET imaging enables assessment of hypoxia as imaged *in vivo.*
- We utilized the CDR (diffusion-convention-reaction) equations, which enable spatial and time-dependent study of the FMISO distribution.
- A sophisticated mathematical approach was utilized to calculate interstitial velocity and pressure, intravascular pressure, as well as oxygen pressure in capillaries and tissues.
- Accurate determination of these parameters is vital to determine some of the parameters in CDR equation
- Blood pressure and oxygen pressure in capillaries are variable.
- We have used 2D vessel configuration, while previous works have used 1D vessel configuration.

Methods

A systematic flowchart is illustrated in Fig. 1 to clarify the computational techniques involved in this work.

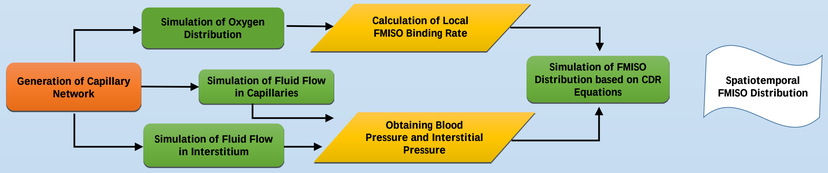

Fig. 1: Flowchart of the simulation process

After the 2D capillary network is created, equations of fluid flow and interstitial flow were simulated in order to determine blood flow and interstitial pressure [1,2,3], which are vital to determine concentration distribution. Details are given by Soltani et al [4].

Then diffusion-reaction equations have been solved for oxygen, to determine [18F]-FMISO local binding rate [5,6]. Therefore having all the parameters of concentration distribution, the CDR equations can be solved based on the following section.

Solute transport:
The general equation for solute transport can be written as [5]:

$$\frac{\partial Cf}{\partial t} = D_{eff}\nabla^2 C_f - \nabla.(V_i C_f) + \Phi_v - \Phi_L$$

$$\frac{\partial c_b}{\partial t} = K_{on} C_f - K_{off} C_b$$

C_f and C_b are free and bound concentration, Φ_v is the rate of solute transport per unit volume from microvessels into the interstitial space, Φ_L is the rate of solute transport per unit volume from the interstitial space into lymphatic vessels, and D_{eff} is the effective diffusion tensor, V_i the interstitial fluid velocity, K_{on} association rate constant and K_{off} dissociation rate constant.

Movement between plasma, free and bounds states is governed by four parameters, L_1, L_2, L_3 and L_4 [5]:

$$L_1 = \left(\frac{L_p S}{V}(P_V - P_t - \sigma_s(\pi_v - \pi_i))(1 - \sigma_f) + \frac{P_m S}{V}\frac{P_e}{e^{Pe}-1}\right)$$

$$L_2 = \left(\frac{P_m S}{V}\frac{P_e}{e^{Pe}-1}\right) + \phi_L$$

$$L_3 = k_{on}$$

$$L_4 = k_{off}$$

$$\phi_L = \begin{cases} \frac{L_{PL} S_L}{V}(P_i - P_L) & \text{normal tissue} \\ 0 & \text{tumor tissue} \end{cases}$$

$$\phi_b = (P_v - P_i - \sigma_s(\pi_v - \pi_i))$$

P_i interstitial fluid pressure, P_v blood pressure in microvessel, S/V the surface area per unit volume of tissue for transport in interstitium, π_v microvessel oncotic pressure, π_i interstitial oncotic pressure, L_p the hydraulic conductivity of the microvessel wall, σ_s osmotic reflection coefficient, $\frac{L_{PL} S_L}{V}$ the lymphatic filtration coefficient, P_L the hydrostatic pressure of the lymphatic, σf is the filtration reflection coefficient and P_m is the microvessel permeability coefficient. Elaborative form of solute transport equation will be as follows:

$$\frac{\partial Cf}{\partial t} = D_{eff}\nabla^2 C_f - \nabla.(V_i C_f) + L_1 C_p - L_2 C_f - L_3 C_f + L_4 C_b$$

$$\frac{\partial c_b}{\partial t} = L_3 C_f - \frac{\partial Cf}{\partial t} = D_{eff}\nabla^2 C_f - \nabla.(V_i C_f) + L_1 C_p - L_2 C_f - L_3 C_f + L_4 C_b$$

Results

The spatiotemporal concentration distribution of [18F]-FMISO at different times is shown in Fig. 2. Free concentration increases up to 600 seconds and decreases afterwards. Bound concentration has an increasing pattern which is promising, since it indicates that [18F]-FMISO accumulates in tissues over time. Fig. 3 shows comparison of average concentration of [18F]-FMISO in tumor region with experimental data [7]. Figure 4 and 5 indicate free and bound concentration variations with time at two points. The trend shows that tracer distribution is highly spatially dependent.

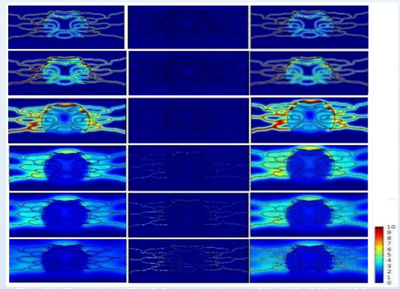

Fig. 2: (From top) FMISO distribution at 60, 120, 600, 1800 , 3600 and 7200 sec . (kBq/ml)

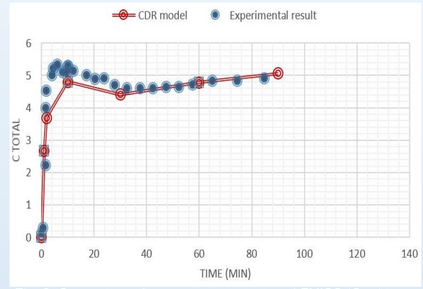

Fig. 3: Comparison of average concentration of FMISO (C_{total}) in tumor region with experimental data

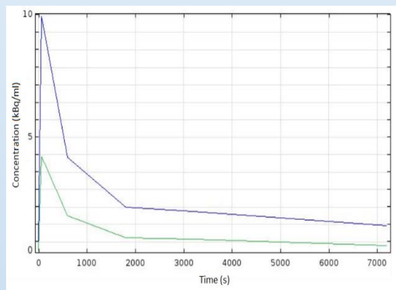

Fig. 4: Free concentration variation with time at two points

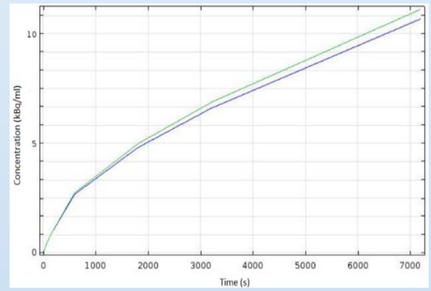

Fig. 5: Bound concentration variation with time at two points

Conclusion

The present work concentrates on the application of convection-diffusion-reaction transposrt phenomena between vessel and tissue as well as within tissue. The results are very close to experimental data, which implies that application of this method in this field is superior to conventional compartment models. This work takes a step forward to bringing the simulation results as close as possible to realistic scenarios. This model accurately predicts radiotracer behavior, i.e. accumulation of the radiotracer in hypoxic regions.

References

1. M. Sefidgar, K. Raahemifar, H. Bazmara, M. Bazargan, S. M. Mousavi, and M. Soltani, *in 2nd Middle East Conference on Biomedical Engineering* 2014,212–215.
2. M. Sefidgar, M. Soltani, H. Bazmara, M. Mousavi, M. Bazargan, and A. Elkamel, *J. Tissue Sci. Eng* 2014, 4,1–8.
3. . T. Stylianopoulos and R. K. Jain, *PANS* 2013, 110,18632–18637.
4. M. Soltani et al., J. Biol. Eng. , 2012, vol. 6, no. 4, p. 4.
5. M. Soltani, M. Sefidgar, M. E. Casey, R. L. Wahl, R. M. Subramaniam, and A. Rahmim, *IEEE Nuclear Science Symposium and Medical Imaging Conference* 2014.
6. D. Monnich, E. G. C. Troost, J. H. A. M. Kaanders, W. J. G. Oyen, M. Alber, and D. Thorwarth, *Phys. INMEDICINE Biol 2012*, 57, 1675–1684.
7. M. Bruehlmeier, U. Roelcke, P. A. Schubiger, and S. M. Ametamey, *J. Nucl. Med* 2004, 45,1851–1859
8. C. J. Kelly and M. Brady, *Phys. Med. Biol* 2006, 51, 5859–5873.